Molecular Biology of the Cell
Vol. 12, 601–614, March 2001

Dynamic Movements of Organelles Containing Niemann-Pick C1 Protein: NPC1 Involvement in Late Endocytic Events[V]

Dennis C. Ko, Michael D. Gordon, Janet Y. Jin, and Matthew P. Scott*

Departments of Developmental Biology and Genetics, Howard Hughes Medical Institute, Beckman Center B300, Stanford University School of Medicine, Stanford, California 94305

Submitted September 12, 2000; Revised December 15, 2000; Accepted January 4, 2000
Monitoring Editor: Monty Krieger

People homozygous for mutations in the Niemann-Pick type C1 (*NPC1*) gene have physiological defects, including excess accumulation of intracellular cholesterol and other lipids, that lead to drastic neural and liver degeneration. The NPC1 multipass transmembrane protein is resident in late endosomes and lysosomes, but its functions are unknown. We find that organelles containing functional NPC1-fluorescent protein fusions undergo dramatic movements, some in association with extending strands of endoplasmic reticulum. In *NPC1* mutant cells the NPC1-bearing organelles that normally move at high speed between perinuclear regions and the periphery of the cell are largely absent. Pulse-chase experiments with dialkylindocarbocyanine low-density lipoprotein showed that NPC1 organelles function late in the endocytic pathway; NPC1 protein may aid the partitioning of endocytic and lysosomal compartments. The close connection between NPC1 and the drug U18666A, which causes NPC1-like organelle defects, was established by rescuing drug-treated cells with overproduced NPC1. U18666A inhibits outward movements of NPC1 organelles, trapping membranes and cholesterol in perinuclear organelles similar to those in *NPC1* mutant cells, even when cells are grown in lipoprotein-depleted serum. We conclude that NPC1 protein promotes the creation and/or movement of particular late endosomes, which rapidly transport materials to and from the cell periphery.

INTRODUCTION

Human Niemann-Pick Type C (NPC) disease is an autosomal recessive lipid storage disorder. The phenotype typically includes organomegaly and progressive neurodegeneration (reviewed in Pentchev *et al.*, 1995). Although the gene responsible for most cases of this disease, *NPC1*, has been cloned (Carstea *et al.*, 1997), its precise function remains a mystery. Cells lacking functional NPC1 accumulate cholesterol in a lysosomal or late endosomal compartment (Blanchette-Mackie *et al.*, 1988; Kobayashi *et al.*, 1999). Normal cells respond to excess cholesterol by reducing synthesis and increasing esterification of cholesterol, but *NPC1* mutant cells fail in this type of homeostasis (Liscum and Faust, 1987; Pentchev *et al.*, 1987).

On the basis of the cholesterol accumulation and other metabolic changes in *NPC1* mutant cells, it has been proposed that the fundamental defect in NPC is a failure to properly transport low-density lipoprotein (LDL)-derived cholesterol out of lysosomes (Pentchev *et al.*, 1984, 1987; Liscum *et al.*, 1989). *NPC1* cells are apparently normal in their internalization and hydrolysis of LDL (Liscum and Faust, 1987), but some evidence indicates that postlysosomal transport of free cholesterol to other intracellular sites is delayed (Sokol *et al.*, 1988; Liscum *et al.*, 1989; Neufeld *et al.*, 1996).

Antibodies have been used to detect NPC1 protein in organelles that contain late endocytic and lysosomal markers such as LAMP2 and Rab7, and that do not contain mannose-6-phosphate receptor (MPR) (Higgins *et al.*, 1999; Neufeld *et al.*, 1999). This localization is consistent with the buildup of cholesterol in late endosomes and/or lysosomes that occurs in NPC disease. The normal function of NPC1 in preventing the buildup is unknown. It has been proposed that NPC1 is present in vesicles that directly transport cholesterol (Liscum and Munn, 1999; Neufeld *et al.*, 1999) but exploring this idea has thus far been restricted to staining fixed cells.

Cholesterol has received the most attention in studies of NPC1, but molecules other than cholesterol may play important roles in NPC1 cell alterations and in disease pathogenesis. The cholesterol-laden organelles in *NPC1* cells also accumulate other lipids and proteins (Watanabe *et al.*, 1998; Kobayashi *et al.*, 1999; Puri *et al.*, 1999). NPC1 mutant cells have a defect in fluid-phase endocytosis, measured using

[V] Online version of this article contains video material for Figure 2–4, 7, and 8. Online version available at www.molbiolcell.org.

* Corresponding author. E-mail address: scott@cmgm.stanford.edu.

[^{14}C]sucrose (Neufeld *et al.*, 1999), indicating that NPC1 may be necessary for a general endocytic process and not cholesterol transport per se. Two recent studies found that transport of LDL-derived cholesterol from lysosomes to the plasma membrane is not blocked in *NPC1* cells (Cruz *et al.*, 2000; Lange *et al.*, 2000). All these results emphasize how much remains to be learned about the function of NPC1 and the molecular basis of NPC pathology.

Aberrant organelle structures and localization remain among the most striking cellular changes in NPC disease. The possible functions of NPC1 in late endosomes or lysosomes, and indeed the detailed properties of NPC1-containing organelles, remain largely unknown. The studies presented here use the approach of monitoring the movements of NPC1-bearing organelles to ask how organelle behavior changes in the absence of functional NPC1. We demonstrate the specific localization of NPC1-FP in a subset of endocytic organelles, track the movements of those organelles, and identify relationships between the NPC1 organelles and other membrane-bound compartments. We show how loss of NPC1 alters the dynamics of organelles in the endocytic pathway and the movement of endocytosed cargo. A temporal description of how these alterations may arise was obtained using a drug that induces changes similar to those caused by loss of NPC1. The results suggest where in membrane and lipid trafficking NPC1 may normally function and raise new questions about the relations between NPC1 and the endoplasmic reticulum (ER).

Understanding the behavior and properties of organelles containing NPC1 will help to address the substantial mysteries of NPC1 function. Resolving the mysteries is critical for understanding the basis of Niemann-Pick disease and devising prevention or treatment strategies.

MATERIALS AND METHODS

Materials

Nocodazole (Biomol, Plymouth Meeting, PA), U18666A (Biomol), Fugene6 (Boehringer-Mannheim, Indianapolis, IN), fluorescent lipids (Molecular Probes, Eugene, OR), filipin (Sigma, St. Louis, MO), and LDL (Sigma) were purchased from commercial sources. F12 and CO_2-independent media were purchased from Life Technologies (Gaithersburg, MD).

Anti-GFP (1:1000; Boehringer-Mannheim), anticaveolin (1:500, Transduction Laboratories, Lexington, KY), anti-PMP70 (1:500; Zymed, San Francisco, CA), anti-βCOP (1:500; Affinity BioReagents, Golden, CO) were purchased from commercial sources. E7 tubulin monoclonal (1:10) and UH1 LAMP-1 monoclonal (1:10) were purchased from the Developmental Studies Hybridoma Bank; Anti-mNPC1 (1:500) was a gift from W.S. Garver (University of Arizona Health Sciences Center, Tucson, AZ), and anti-MPR was a gift from S.R. Pfeffer (1:500) (University of Iowa, Iowa City, Iowa). Sec61β-FP and T2-FP were a gift from J. White; VAMP7-FP was a gift from R. Advani (Stanford University, Palo Alto, CA). CHO-KI and PtK2 cells were purchased from American Type Cell Culture (Manassas, VA). CT60 and 25RA CHO cells were a gift from T.Y. Chang (Dartmouth University, Hanover, NH).

Construction and Expression of NPC1-FP

The mouse cDNA to NPC1 was provided by S. Loftus. Annealed oligonucleotides from the Eco47III site to the end of the open reading frame were used to replace the stop codon and add a 6xHis tag and *Kpn*I site. The modified cDNA was ligated into the *Xho*I and *Kpn*I sites of pEGFP-N3, pEYFP-N3, and pECFP-N3 (Clontech, Palo Alto, CA). A *Not*I fragment containing the mNPC1-FP fusion was introduced into the *Not*I site of pCEP4 to allow for selection with hygromycin. The cytomegalovirus promoter was used to drive expression.

Transfections with Fugene6 were carried out according to manufacturer's suggestions. For assessment of cholesterol clearance, cells were fixed with 3% paraformaldehyde, stained with filipin (50 μg/ml) for 1 h, and scored for complementation 48 h after transfection.

Stably expressing cells were selected with hygromycin (250 μg/ml). Postnuclear supernatants were resolved on 4–12% gradient gels, blotted, and probed with anti-green fluorescent protein (GFP) to detect expression. Stably expressing cells stained with filipin were indistinguishable from 25RA cells, the line from which CT60s are derived.

Point mutations in NPC1-FP were introduced using Quikchange (Stratagene, La Jolla, CA). We made five different point mutations (C64S, C98S, Y635C, Y635A, P692S) that had been reported to result in a nonfunctional NPC1 localized to the correct compartment (Watari *et al.*, 1999a,b). In our experiments four of the mutant NPC1-FPs became concentrated primarily in the ER, a behavior typical of incorrectly folded proteins. C98S and Y635C localized correctly in a subset of cells, but each of these mutants had residual function; examination of cells 2 to 3 d posttransfection demonstrated at least partial clearing of accumulated cholesterol in a fraction of the cells. The fifth mutant, P692S, had minimal function after 2 d (only ~5% of the cells display partial clearing), and was correctly located in about half of the cells, as determined by comparison to LAMP1 localization.

Immunofluorescence Microscopy

Cells were grown in chamber slides (Nalge Nunc International, Rochester, NY), fixed in 3% paraformaldehyde, permeabilized, and blocked with either 0.05% saponin or filipin and 10% normal goat serum, and stained with primary antibody overnight in permeabilization/blocking solution with 0.1% azide. Cells were washed three times with phosphate-buffered saline and stained with the appropriate CY5-conjugated secondary antibody for 1 h. Cells were washed again and mounted with VectaShield (Vector Labs, Burlingame, CA).

Cells were imaged using a Zeiss Axiovert S100TV with a 100×/1.40 Plan NeoFluar objective, MicroMax 1800Y charge-coupled device camera (Princeton Instruments, Trenton, NJ), and MetaMorph software (Universal Imaging, Media, PA). Sequential images were taken using fluorescein isothiocyanate and CY5 filters (Chroma, Brattleboro, VT) and overlayed to determine colocalization. For antibodies with significant perinuclear staining (MPR, βCOP), images were acquired using a Bio-Rad (Richmond, CA) MRC 1024 confocal microscope.

Live Cell Imaging and Analysis

Cells were grown in chambered cover glasses (LabTek) and just before imaging, the media were changed to CO_2-independent media with 10% fetal calf serum. Cells were imaged using the epifluorescence microscope described above. Temperature was maintained at 37°C by using a heater blower device (constructed in-house by D. Proffitt) and a Plexiglas environmental chamber (M&Ko, Union City, CA).

Time-lapse imaging was performed using filters controlled by Lambda10 shutter drivers (Sutter, Novato, CA). For dual CFP/YFP imaging, separate excitation and emission filters (JP4 set; Chroma) were used to take two rapid sequential images at each time point. Stacks of time-lapse images were analyzed using MetaMorph. For tracking of a random sample of particle movements, 20 markers

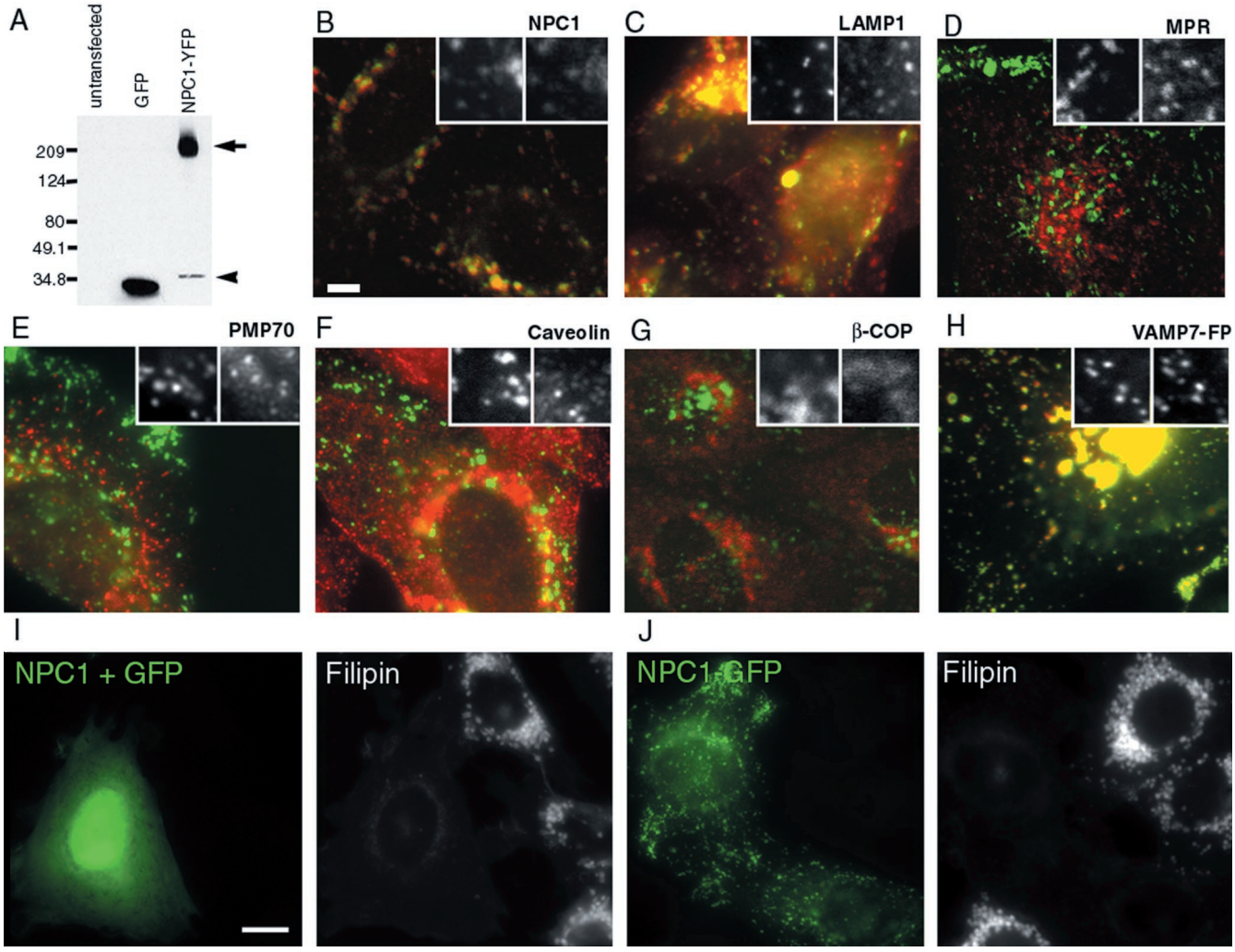

Figure 1. NPC1-FP is correctly localized in CT60 CHO cells and is functional in clearing accumulated cholesterol. Extracts of CT60 cells expressing GFP or NPC1-YFP were resolved on a 4–12% gradient gel and probed with an anti-GFP antibody (A). The NPC1-YFP stable line produces predominant bands near 200 kDa (arrow), consistent with the glycosylated forms of NPC1-YFP (predicted molecular weight for nonglycosylated fusion = 170 kDa). A faint smaller band (arrowhead), presumably a cleavage product, is also present, but the colocalization of NPC1-GFP with anti-NPC1 antibody staining (B) indicates that the tag stays largely attached to NPC1. Bar, 5 μm. Cells expressing NPC1-YFP were antibody stained with various primary antibodies, followed by incubation with CY5-conjugated secondary antibody, and imaged using the appropriate filter sets. The tagged protein localizes to organelles that contain LAMP1 (C) but do not contain the cation-independent MPR (D). To determine whether the protein is localizing only to this compartment, other markers were examined, including PMP70 (E), caveolin (F), βCOP (G), and VAMP7-FP (H). CT60 cells were transiently transfected with NPC1 and GFP (I) or NPC1-GFP (J) and the amount of free cholesterol was evaluated by filipin staining in each case. NPC1-GFP is able to clear the accumulated cholesterol as well as untagged NPC1 (97 $\pm$ 1 versus 95 $\pm$ 2% of expressing cells rescued). GFP alone has no affect on the accumulated cholesterol (3.5 $\pm$ 0.5%). Bar, 5 μm.

were randomly placed on images of cells. The fluorescent structure closest to each marker was manually tracked for 10 s by using the TrackPoints command of MetaMorph. To determine the percentage of total particles undergoing vectorial movements, all particles in a cell over a 10-s period were categorized based on displacement $>$ or $<$1.5 μm. For quantification of movement to and from the perinuclear aggregate, streaming acquisition was used for 30 s and the total number of events was counted. P values for statistical significance were measured using the *t* test for nonpaired data.

Over short time periods ($<$10 min), fluorescence imaging had no effect on the motility or localization of NPC1-FP organelles. Some aggregation of NPC1-organelles, similar to that seen with U18666A treatment, occurred with cells irradiated for 2 h. However, all NPC1-FP–producing cells treated with U18666A had perinuclear aggregates even if they were not irradiated during the 2 h.

DiI LDL Time Course

Cells were washed with F12 (10% lipoprotein-deficient serum [LPDS]) and then labeled for 3 min at 37°C with F12 (10% LPDS) with 30 μg/ml DiI LDL. This short pulse was followed by a variable chase period in F12 (10% LPDS + 50 μg/ml LDL) at 37°C. Following

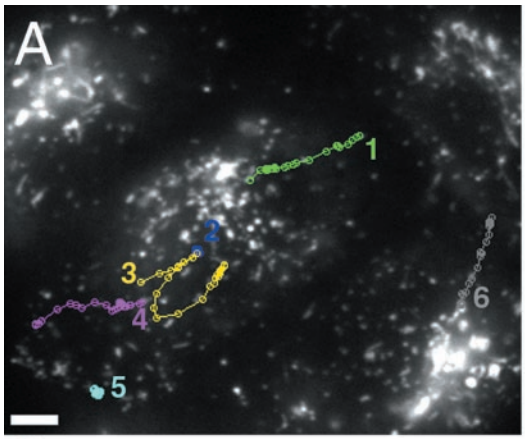

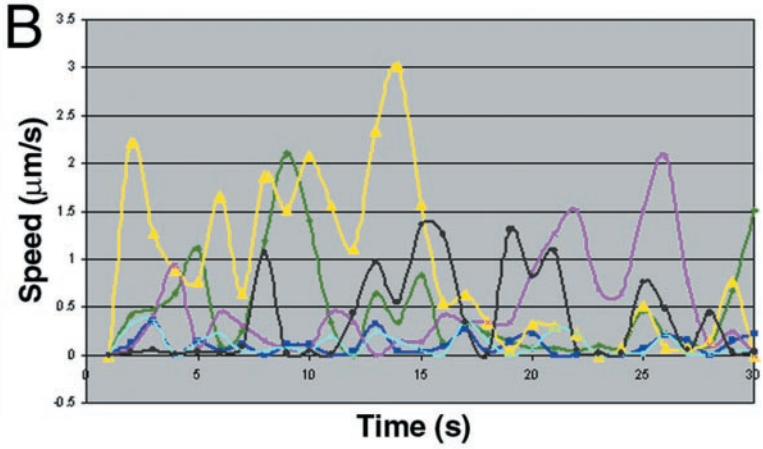

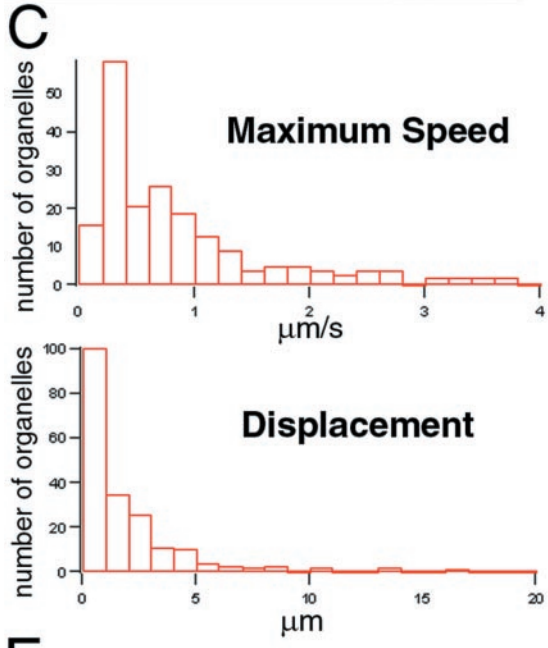

D

Movement of NPC1 Organelles Over A 10s Period	
Number of cells	10
Number of organelles tracked	200
Organelles with displacement >1.5μm	77
Mainly plus-end directed	34
Mainly minus-end directed	26
Average Maximum Speed	1.57 (+/-0.88) μm/s
Range of Speeds	0.45-3.8 μm/s

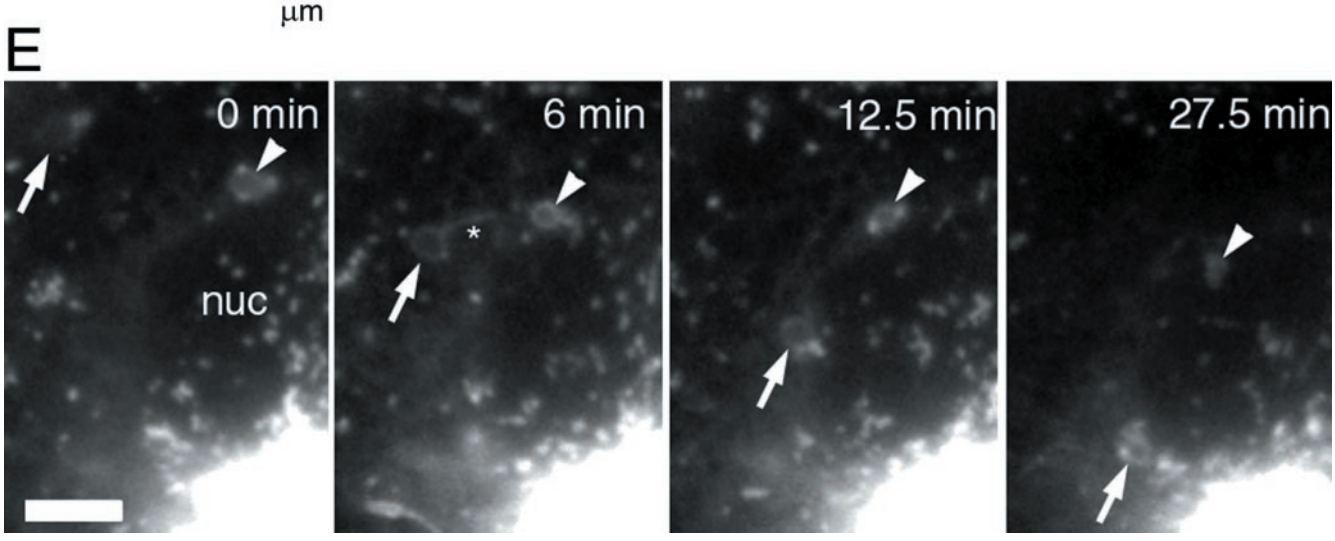

Figure 2.

this period, cells were washed with phosphated-buffered saline and fixed for 10 min with 3% paraformaldehyde. Images were acquired using confocal microscopy. For assessment of motility, live cells were imaged as described above at the indicated times.

Online Supplemental Material

Quicktime movies that accompany many of the figures are available at the MBC Web site.

RESULTS

Functional Integrity of NPC1-FP

To follow NPC1 in living cells, sequences coding for the fluorescent proteins EGFP, EYFP, or ECFP were fused in frame to the C terminus of mouse NPC1. The genes were expressed in CT60 cells, Chinese hamster ovary (CHO) cell derivatives that carry null mutations in *NPC1* (Cadigan *et al.*, 1990; Cruz *et al.*, 2000). Antibodies against GFP detect a band of ~200 kDa in blotted protein extracts from stably transfected NPC1-FP cells, consistent with the expected size for the glycosylated form of an intact NPC1-FP protein (Figure 1A).

Previous studies have shown that NPC1 protein is located in organelles that contain late endocytic and lysosomal markers (LAMP-2 and Rab-7) but do not contain MPR (Higgins *et al.*, 1999; Neufeld *et al.*, 1999). Most of the NPC1-FP organelles colocalized with the late endosomal/lysosomal marker LAMP-1 (Figure 1C) and not with the *trans*-Golgi, late endosomal marker MPR (Figure 1D), the peroxisomal marker PMP70 (Figure 1E), caveolin (Figure 1F), or the Golgi marker βCOP (Figure 1G). Nearly all NPC1-FP containing organelles, organelles ~0.5–1.5 μm in size with tubules up to 7 μm in length, could also be labeled with VAMP7-FP (Figure 1H), a marker of late endosomes/lysosomes (Advani *et al.*, 1998, 1999). An additional population of small structures (≥500 nm) contained VAMP7-FP but not NPC1-FP. All of these established criteria indicate that the NPC1-FP protein is correctly targeted to a late-endosomal and/or lysosomal compartment.

The aberrant cholesterol metabolism of CT60 cells can be restored to a largely normal state by complementation with *NPC1* (Watari *et al.*, 1999a; Cruz *et al.*, 2000), so the effects of the fluorescent protein tags on function were assessed with this assay. In CT60 cells, free cholesterol accumulates in large abnormal vesicles (1–3 μm) that can be labeled with the fluorescent antibiotic filipin (Cadigan *et al.*, 1990). Following transient transfection, nearly all cells expressing either untagged NPC1 (95 ± 2%; Figure 1I) or NPC1-FP (97 ± 1%; Figure 1J) had an unequivocal decrease in cholesterol content compared with nontransfected cells in the same culture or cells transfected with GFP alone (3.5 ± 0.5%; our unpublished results). Thus, the NPC1-FP plasmids produced intact fusion proteins that resemble the endogenous NPC1 protein in function and localization.

NPC1-FP Organelles Participate in Three Kinds of Movements

The proper function and localization of NPC1-FP provided an opportunity to meaningfully observe movements of organelles containing NPC1-FP. In stably transfected CT60 cells, three types of NPC1-FP–containing organelle movements occurred. We refer to the types of movement as vectorial, Brownian, and slow retraction (Figure 2 and videos 1 and 2).

The most striking movements of the NPC1 organelles were rapid vectorial movements (Figure 2A, tracks 1, 3, 4, and 6; video 1). Vectorial movement primarily followed paths either toward or away from the nucleus, often between relatively stable perinuclear and peripheral aggregates of NPC1-containing membranes. During a 10-s period, ~39% of NPC1-FP organelles engaged in vectorial movements with a displacement of >1.5 μm (Figure 2D). Roughly equal numbers moved toward or away from the nucleus; some individual organelles rapidly changed direction. Speeds ranged from 0.45 to 3.8 μm/s. Vectorial movements are dependent upon, and follow, microtubules (Ko and Scott, unpublished data). Similar distribution and dynamics were observed in several other fibroblast and epithelial cell types, including, CHO-KI, 10T1/2, SW13, MDCK, and PtK2.

Most NPC1-bearing organelles also underwent apparent Brownian movements, short continuous back-and-forth movements with little if any translational movement (Figure 2A, tracks 2 and 5). These movements continued after the cytoskeleton was disrupted with 40 μM nocodazole (our unpublished results). NPC1-FP–containing organelles intersperse vectorial movements with longer periods of only Brownian movement (Figure 2B), as do lysosomes labeled with acridine orange (Herman and Albertini, 1984; Matteoni and Kreis, 1987).

The third type of movement, slow retraction, is observed during longer time-lapse experiments. Large (~2 um) NPC1-positive "rings," the rings being cross-sectional views of organelles with NPC1 on their surfaces, move toward the nucleus at ~0.01 μm/s. Usually, 0–3 such rings were present in each cell. The rings moved toward the nucleus while undergoing a simultaneous reduction in diameter (Figure 2E; video 2). Numerous smaller NPC1-containing organelles moved rapidly along the surfaces of these rings

Figure 2 (facing page). NPC1-FP localizes to moving structures that are variable in their rates and direction. NPC1-FP was observed in punctate and tubulovesicular structures that moved both toward and away from the perinuclear region at a broad range of speeds. The paths of several structures over 30 s are shown in A, with the number of the path next to the organelle's initial position. The instantaneous speeds of the tracked particles are plotted versus time, demonstrating the stop-and-go nature of the movements (B). We examined the movements of 200 randomly chosen structures from 10 cells and characterized the movements based on maximum speed, displacement, and direction (C and D). Large NPC1-FP rings move toward the nucleus while simultaneously decreasing in size (E). Images taken every 30 s for 30 min revealed that structures that appeared stably localized over shorter intervals, undergo a retraction toward the perinuclear region. Two retracting rings are pointed out with an arrow and arrowhead. Note the changing tubular structures extending from the rings, particularly at 6 min (asterisks). Bar, 5 μ m. Video 1 accompanies Figure 2A. NPC1-FP localizes to moving structures that are variable in their rates and direction. Images were acquired every second for 30 s and played back at a rate of six images per second. Video 2 accompanies Figure 2E. Slow retraction of large NPC1-FP rings. Images were acquired every 30 s for 30 min and played back at a rate of six images per second.

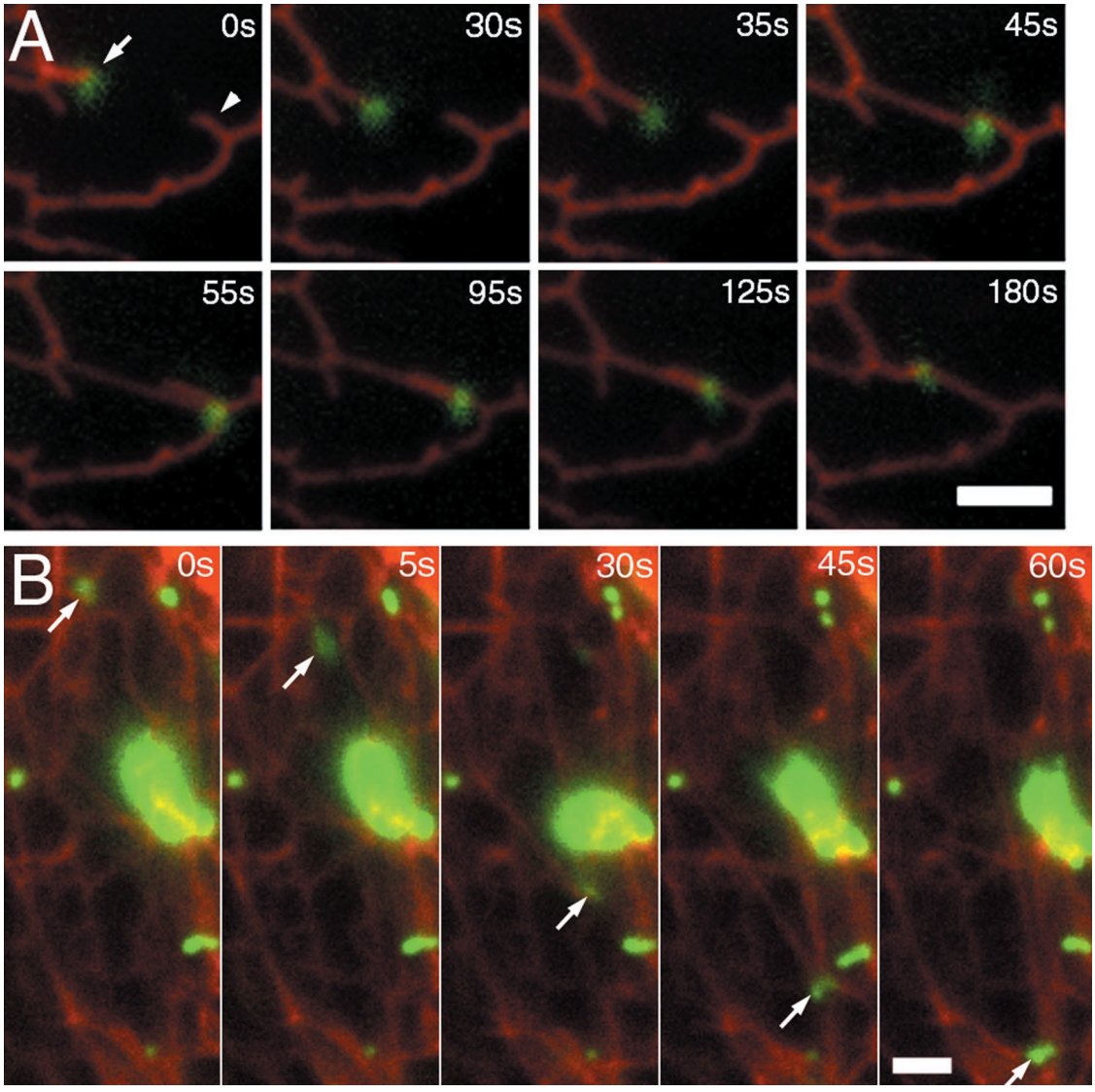

Figure 3. NPC1-FP vesicles associate with and move with the ER. CT60 cells stably transfected with NPC1-YFP were transiently transfected with Sec61beta-CFP, an ER-resident protein. Twenty-four hours posttransfection, the two proteins were visualized by sequential exposures (0.5 s CFP and 1 s YFP) taken every 5 s. Images at each interval were merged and the relative motions of the labeled structures were examined. (A) The eight frames show an organelle with NPC1-YFP that is localized at the end of an ER segment (arrow). The two move a distance of ~3 μm to associate with another ER segment (arrowhead) (0–55 s). The vesicle and ER then appear to retract along this second segment of ER until resting at the junction between the two segments (55–180 s). (B) An NPC1-FP organelle (arrow) moves a distance of ~16 μm while pulling a segment of ER with it. Bar, 2 μm. Video 3 accompanies Figure 3A. NPC1-YFP organelles associate with the ends of ER segments labeled with Sec61β-CFP. Sequential CFP and YFP images were acquired every 5 s for 3 min and played back at a rate of six images per second. Video 4 accompanies Figure 3B. NPC1-YFP organelles appear to pull middle segments of ER labeled with Sec61β-CFP. Sequential CFP and YFP images were acquired every 5 s for1 min and played back at a rate of six images per second.

and also engaged in vectorial movement to and from the rings.

NPC1 Organelles Interact with the ER

The dramatic movements of NPC1 organelles are suggestive of a role in directed transport of cargo such as LDL-derived cholesterol. Loss of NPC1 function has been linked to delayed transport of cholesterol to the ER and plasma membrane (Sokol *et al.*, 1988; Liscum *et al.*, 1989; Neufeld *et al.*, 1996), so we looked for evidence of fusion between NPC1 organelles and the ER or plasma membrane. Fusion of post-Golgi transport "containers" with the plasma membrane has been demonstrated in thin PtK2 cells for VSVG3-GFP (Toomre *et al.*, 1999). NPC1-FP organelles did not undergo the characteristic docking and rapid disappearance reported for VSVG3-GFP, based upon observing many cells for peri-

ods >10 min. NPC1-FP organelles are often located near the Golgi, but two-color observations by using the marker T2-FP (Storrie *et al.*, 1998) did not reveal any clear interaction (our unpublished results).

In contrast, a close apposition between the ER and NPC1 organelles was observed repeatedly. The ER was labeled with Sec61β-FP (Rolls *et al.*, 1999). NPC1-containing organelles were present at the ends of ER strands and move with the strands as they extend (Figure 3A; video 3). Some NPC1 organelles moved long distances (up to 20 μm) while seemingly pulling against the middle of a segment of ER; the resultant force caused a distortion in the shape of the NPC1 organelle (Figure 3B; video 4). The rapid bleaching of fluorescent lipids (BODIPY-lactosylceramide, BODIPY-sphingomyelin) made any transfer of fluorescent lipids between NPC1 organelles and the ER difficult to observe, so whether such transfers occur remains an open question.

Cells Lacking Functional NPC1 Have Reduced Vectorial Movement of NPC1-FP Organelles

NPC1 function is required for the vectorial movements of NPC1-containing organelles. For these experiments we marked the NPC1 compartment in *NPC1* mutant cells (CT60 cells) with nonfunctional NPC1 protein. Of five mutant NPC1-FP constructs (see MATERIALS AND METHODS), P692S was chosen as the best available marker of the normal NPC1-containing compartment in cells lacking functional NPC1. As a second way of tracking relevant cell compartments, the movement of VAMP7-FP was followed in CT60 cells. VAMP7-FP is normally located in the same organelles as NPC1, as well as in many tiny vesicles that have no detectable NPC1. By following movements of the large VAMP7-containing organelles in CT60 cells, we observed how the distribution and movements of organelles that normally contain NPC1 were altered by the absence of functional NPC1.

The lack of functional NPC1 severely affected vectorial movements. Brownian movements, slow retraction, and some movements in close association with the ER continued in cells that had no functional NPC1 (our unpublished results), but vectorial movements were strikingly reduced (Figure 4). Most movements of organelles containing VAMP7-FP, followed during 60-s periods, consist of short forays without a clear direction (Figure 4A; video 5). Data from tracking 100 organelles show a decrease in both maximum speed (mean = 0.31 $\pm$ 0.32 versus 0.84 $\pm$ 0.82 μm/s; $p < 0.0001$) and displacement (mean = 0.50 $\pm$ 0.64 versus 1.8 $\pm$ 2.5; $p < 0.0001$) during a 10-s interval (Figure 4B). In mutant cells drastically fewer organelles undergo vectorial movement (Figure 4C), which is not due to a reduced number of the organelles. We find on average 130–160 organelles/cell with or without functional NPC1, although in NPC1-expressing cells the number is probably an underestimate due to local aggregations. In NPC1-YFP stably expressing cells, 37% ($\pm$4%) of all NPC1 organelles are engaged in vectorial movement during a 10-s period. In CT60 cells far fewer organelles with VAMP7-FP or P692S NPC1-CFP moved, 4.4% ($\pm$1.7%; $p < 0.0001$) and 7.7% ($\pm$4.6%; $p < 0.0001$), respectively.

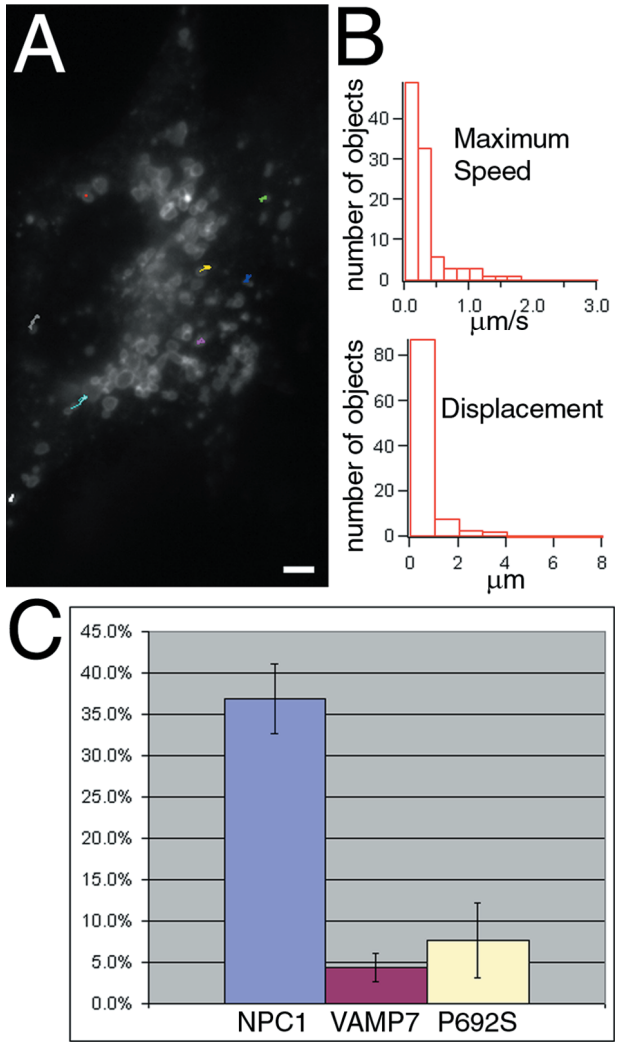

Figure 4. NPC1-containing organelles display reduced movement in cells lacking functional NPC1. To monitor the movements of the NPC1-containing compartment in cells lacking functional NPC1, VAMP7-FP or NPC1(P692S)-FP was transiently transfected into CT60 cells to mark the abnormal organelles. Representative tracks for VAMP7-FP are shown in A. Quantification of the movement of 100 randomly chosen organelles from five cells (B) shows that the speed and displacement of these organelles are severely decreased in CT60 cells. Observations of all the fluorescent organelles within cells showed that the fraction engaged in vectorial transport is decreased in cells lacking functional NPC1 or expressing an NPC1 mutant with reduced function (P692S) (C). Bar, 5 μ m. Video 5 accompanies Figure 4A. Reduced movement of VAMP7-FP organelles in *NPC1* mutant cells. Images were acquired every second for 1 min and played back at a rate of six images per second.

NPC1-bearing Organelles Participate in Late Events in the Endocytic Pathway

The reduced organelle movements in *NPC1* mutant cells could reflect either a requirement for NPC1 in motility or the shifting of NPC1 into a nonmotile compartment. Evidence for the second possibility was obtained in pulse-chase ex-

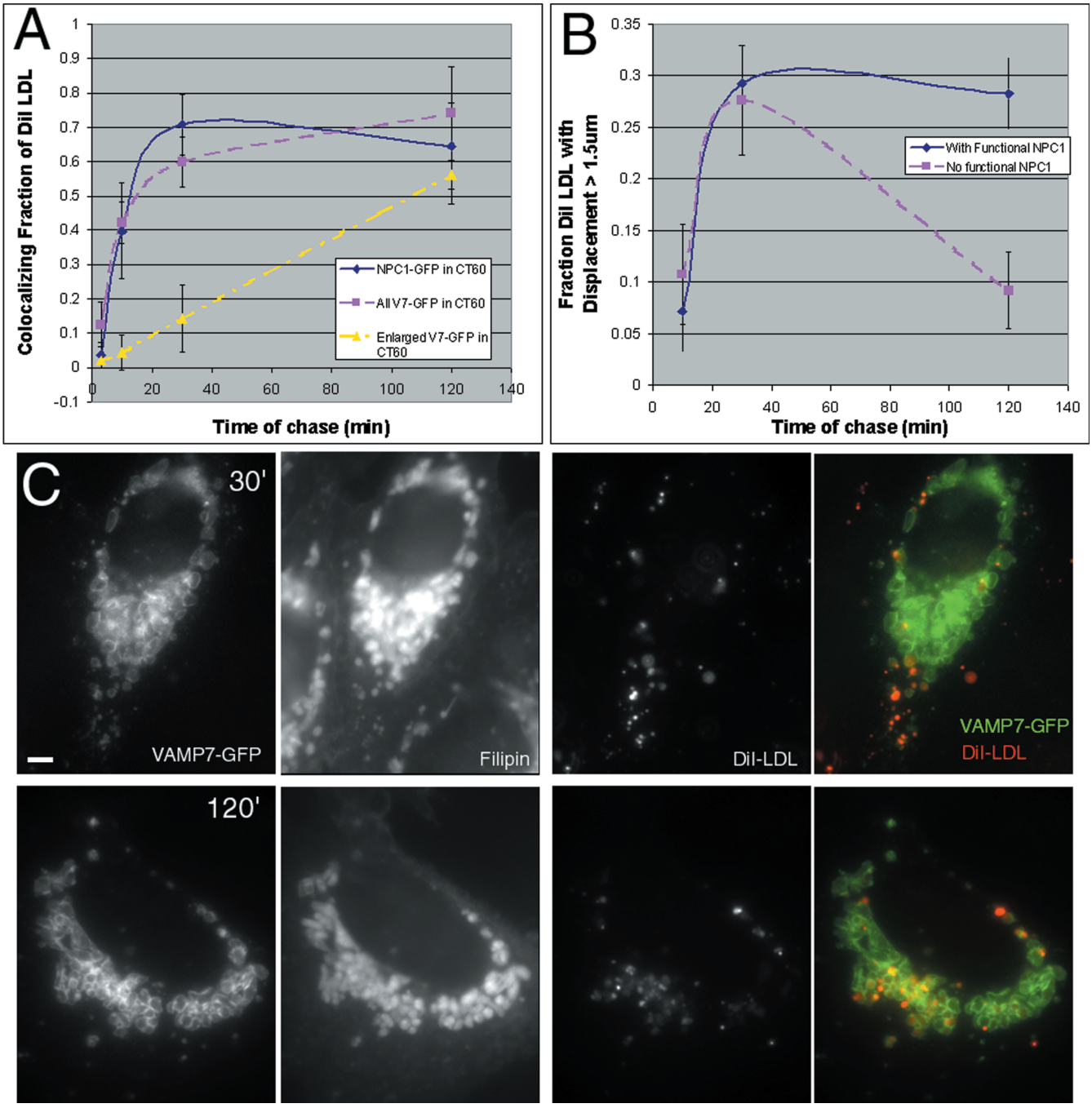

Figure 5. NPC1-FP organelles participate in late events in the endocytic pathway. Pulse-chase experiments at 37°C with DiI LDL revealed the kinetics of entry into the NPC1-containing compartment. CT60 cells transiently transfected with NPC1-GFP or VAMP7-GFP were labeled with DiI-LDL (30 μM) for 3 min and then fixed following a 3-, 10-, 30-, and 120-min chase period. The fraction of all DiI-labeled structures that colocalized with NPC1-GFP, VAMP7-GFP, or only the enlarged VAMP7-GFP organelles was quantified for 10 cells at each time point (A). DiI shows significant colocalization with NPC1-GFP or VAMP7-GFP at 10 min and later time points, indicative of NPC1-FP being present in late endosomes and the terminal endocytic compartment. The enlarged VAMP-GFP organelles colocalize with DiI beginning at 30 min, but the bulk of the DiI has not reached these organelles until 2 h (C). In living cells, the fraction of all DiI-labeled structures engaged in vectorial movement (displacement >1.5 μm) was quantified at 10, 30, and 120 min (B). Similar amounts of movement were seen early in the endocytic pathway (10 and 30 min) regardless of the presence of NPC1. Following these normal early movements, loss of NPC1 prevents further DiI movement (2 h) and results in the sequestration of DiI in the cholesterol-laden organelles. Bar, 5 μm.

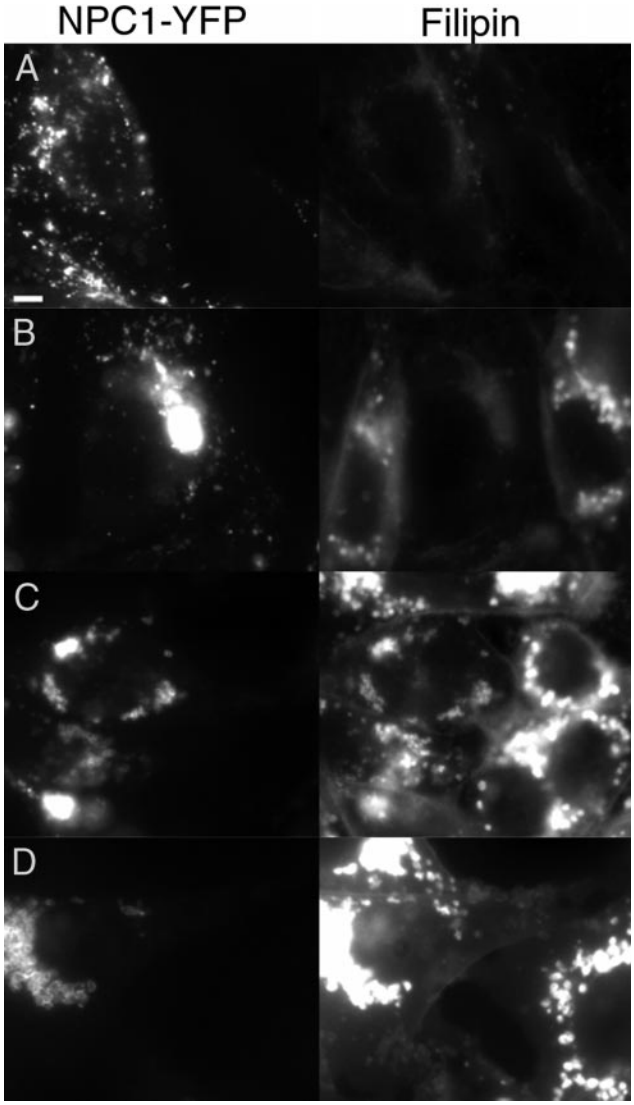

Figure 6. Overexpression of NPC1 results in decreased sensitivity to U18666A. NPC1-YFP expressing cells were plated with 25RA cells and treated for 24 h with 0, 0.3, 3, and 10 μM U18666A (A–D). YFP fluorescence is shown on the left and filipin staining on the right. The low concentration of U18666A (0.3 μM) is able to induce cholesterol accumulation in 25RA cells but not in the cells overexpressing NPC1-YFP. Increasing the U18666A is able to overcome this suppression, as shown with intermediate (3 μM) and high concentrations (10 μM) of the drug. Bar, 5 μm.

periments monitoring DiI LDL movement through the endocytic pathway.

DiI LDL uptake rates serve to identify specific organelle compartments and can show which compartments contain NPC1. Following a brief pulse with DiI LDL (30 μg/ml for 3 min), cells were fixed at various times and the distributions of NPC1-FP and DiI were compared (Figure 5A). After a 3-min chase period, DiI is in a compartment, presumably early endosomes, which does not contain NPC1. After 10 min nearly half of the DiI colocalized with a subset of NPC1-containing structures. This is consistent with some of the NPC1-FP organelles being late endosomes, because DiI LDL enters this compartment with a half-time of 8 min in CHO cells (Salzman and Maxfield, 1989). Colocalization increased to ~70% of the DiI at 30 min; this degree of colocalization remained fairly constant for the ensuing 2 h, indicating that NPC1-FP is also present in the terminal compartment. At these later time points, the LDL has disintegrated (Ohashi *et al.*, 1992), but the DiI continues to serve as a membrane marker. From these experiments it appears that NPC1-FP is present in both late endosomes (colocalizing with DiI at ~10 min) and the terminal endocytic compartment (colocalizing with DiI from ~30 min onward). The terminal compartment is traditionally called a lysosome but is perhaps more accurately described as a late endosome/lysosome hybrid (reviewed in Luzio *et al.* 2000).

In *NPC1* mutant cells, enlarged organelles accumulate, and DiI LDL uptake identifies them as the terminal endocytic compartment or an aberrant compartment with no simple equivalent in a normal cell. DiI LDL enters VAMP7-positive organelles, i.e., organelles that normally contain NPC1, with similar kinetics in the presence or absence of functional NPC1. Therefore, early events in the endocytic pathway do not require NPC1 function. In wild-type cells, 30 min of DiI LDL uptake puts 70% of the label in late endosomes and the terminal compartment, but in cells without functional NPC1, only ~15% of the structures labeled with DiI were enlarged organelles and most of these were near the cell periphery (Figure 5C). By 2 h, most of the DiI signal was found within the lumen of the perinuclear cholesterol-laden organelles (Figure 5C) and this did not change even following an 18-h chase (our unpublished results). This delayed and persistent colocalization of the enlarged organelles and DiI indicates that the organelles are the terminal endocytic compartment or an intermediate arrested after the late endosome step of the endocytic pathway.

The relationship between endocytic compartments and the decreased vectorial movements seen in *NPC1* mutant cells was revealed by live cell imaging following variable chase periods. In cells with functional NPC1-FP, nearly 30% of DiI-labeled organelles were engaged in vectorial movements after a 2-h chase. In cells lacking functional NPC1, <10% of the DiI was engaged in vectorial movement at the same time point. The lack of NPC1 causes DiI to become sequestered in enlarged organelles with reduced motility. Earlier time points (10 and 30 min) show that the movement of DiI LDL is initially indistinguishable between normal and NPC1 mutant cells (Figure 5B). This suggests that deliveries from early endosomes to late endosomes and from late endosomes to the terminal compartment are normal in NPC1 mutant cells. Functional NPC1 allows DiI-labeled organelles to reach the terminal compartment and then continue to move between perinuclear and peripheral locations, perhaps recycling late endosomal and/or lysosomal membranes for more rounds of endocytosis. Cells lacking functional NPC1 accumulate DiI in enlarged terminal endocytic organelles that remain sequestered in the perinuclear region. This trapping process, a failure of DiI cycling, follows successful early inward movements of organelles that carry DiI LDL.

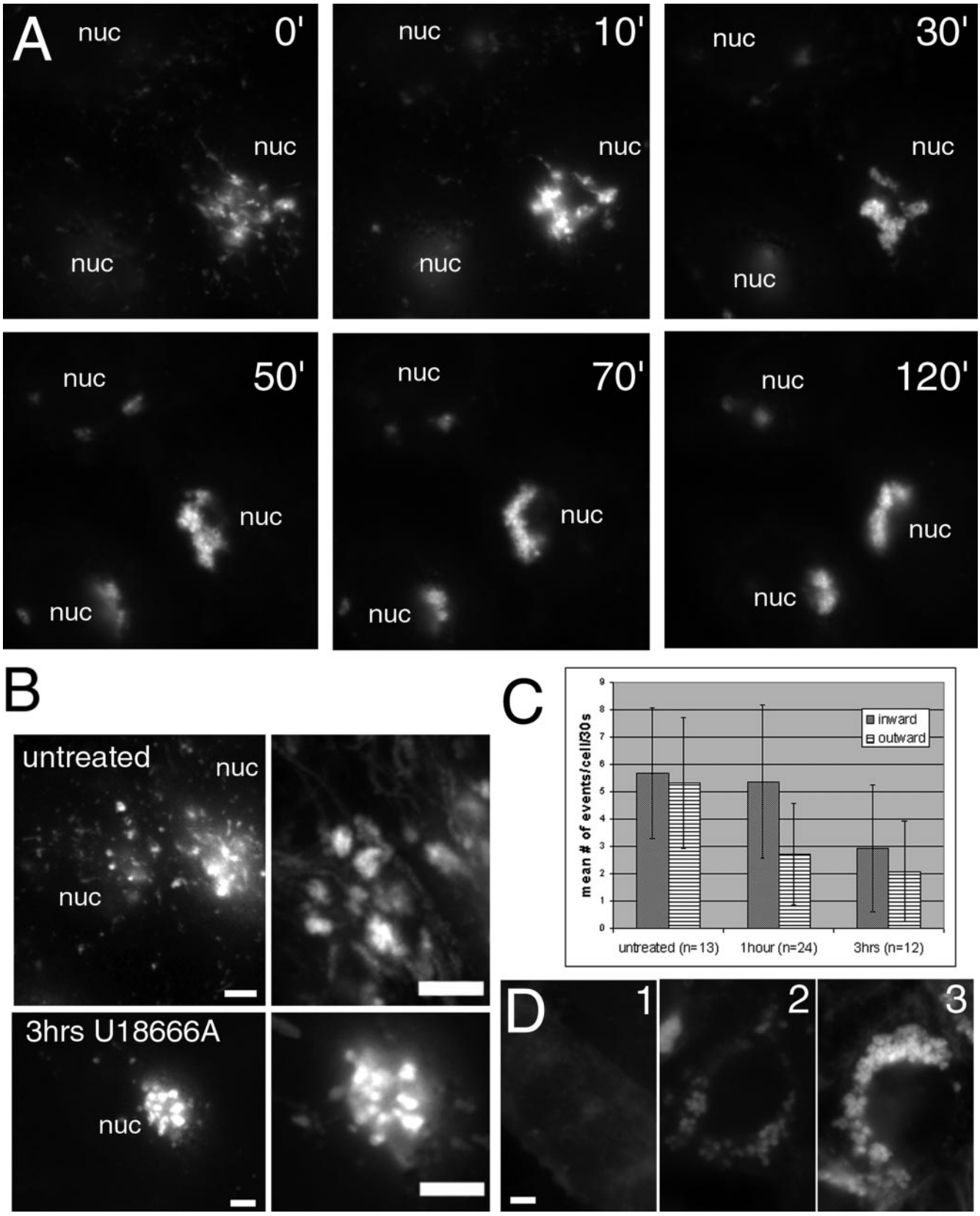
A
nuc
0'
10'
30'
50'
70'
120'
B
untreated
3hrs U18666A
C
mean # of events/cell/30s
inward
outward
untreated (n=13)
1hour (n=24)
3hrs (n=12)
D
1
2
3

Figure 7.

U18666A Alters the Dynamics of Perinuclear NPC1 Organelles

To observe the sequence of changes that results in membrane accumulation in the terminal compartment, we used a drug that causes *NPC1*-like cholesterol accumulation. Recent studies suggest that class 2 amphiphiles, such as U18666A, act upon NPC1 or in the same pathway (Lange *et al.*, 2000). We tested the relation between NPC1 and the class 2 amphiphiles by seeing whether overexpression of NPC1 suppresses the accumulation of cholesterol induced by the drugs. U18666A induces partial cholesterol accumulation at doses as low as 30 nM in 25RA cells, the parental line of CT60 (Cadigan *et al.*, 1988). In contrast, NPC1-YFP–producing cells treated with this concentration (and up to 1 μM) have filipin staining that is indistinguishable from untreated cells (Figure 6B). At a 100-fold increase in concentration (3 μM), the cells accumulate cholesterol to a level intermediate between untreated cells and treated 25RA cells (Figure 6C). At higher concentrations (10 μM), NPC1-YFP–expressing cells are no longer resistant to the U18666A treatment (Figure 6D). Similar results were obtained in CHO-KI cells overexpressing NPC1-YFP (our unpublished results). NPC1-YFP–expressing cells are resistant to induction of cholesterol accumulation by another class 2 amphiphile, progesterone (Butler *et al.*, 1992). In 25RA control cells, 1 μM progesterone causes cholesterol accumulation, whereas accumulation in NPC1-YFP–expressing cells requires ~100-fold more (our unpublished results). These results provide further evidence that the class 2 amphiphiles affect NPC1 or a closely related cell function.

By monitoring the changes induced by U18666A over time, we observed alterations in NPC1 organelle movements that preceded the bulk of cholesterol accumulation. During the first 2 h after addition of U18666A to 10 μM, tubular extensions decrease while aggregation of perinuclear NPC1 organelles increases (Figure 7A; video 6). The size of the organelles that contribute to the aggregate increases with continued incubation, presumably as more membrane is delivered to the organelles.

Such a dramatic change in NPC1-FP organelle localization could be caused either by increased transport into the perinuclear region or by elimination of vectorial transport of NPC1-FP organelles out of the more stationary perinuclear NPC1-FP organelles. Short time-lapse images (30 s) were examined following a 2- to 3-h incubation with U18666A. In contrast to the many rapidly moving, small, perinuclear organelles in untreated cells, few organelles engaged in vectorial movement to and from the perinuclear aggregate following this incubation (Figure 7B; video 7 and 8). We measured movements at 1–1.5 h and 2.5–3.5 h after U18666A introduction. At the earlier time point the number of inward directed events remained the same, while outward movements were decreased (2.7 ± 1.8 versus 5.3 ± 2.4 outward events/cell/30 s; $p < 0.0008$). During the later time interval, both directions of movement were severely decreased, presumably because most of the NPC1 organelles were now in the aggregate (Figure 7C). We conclude that U18666A inhibits the movement of organelles toward the cell periphery, causing their accumulation in the perinuclear region.

U18666A had its effects regardless of the presence or absence of LDL. Cells grown for 48 h in media with 10% LPDS, or no serum, still formed enlarged perinuclear NPC1 organelles when incubated with U18666A for the last 24 h, though the overall level of filipin fluorescence was less than in cells grown in media with normal LDL levels (10% fetal bovine serum) (Figure 7D). Even when grown with LPDS the cells had perinuclear aggregates after 4 h of incubation with U18666A (our unpublished results). This suggests that LDL-derived cholesterol is cargo that accumulates in organelles that lack functional NPC1; the aberrant organelles form regardless of LDL import.

Figure 7 (facing page). The formation of cholesterol-laden organelles in cells treated with U18666A. Cells were incubated with 10 μM U18666A and imaged every 30 s for the first 2 h of treatment (A). By 2 h, all cells displayed a prominent perinuclear aggregate formed from the loosely associated, dynamic perinuclear cluster of NPC1 organelles present in untreated cells. (B) Images (100) taken over 25 s have been merged to show the tracks of movement into and out of this perinuclear cluster in untreated cells and cells treated for 3 h with U18666A. Quantification of the movement to and from the perinuclear aggregate (C) reveals decreased movement out of the aggregate at 1–1.5 h and decreased movement in both directions by 2.5–3.5 h. The effects of U18666A did not require the presence of exogenous sources of cholesterol as shown by filipin staining in D. Cells incubated in F12 without serum for 48 h (D1) still formed enlarged cholesterol-laden organelles when incubated for the final 24 h with U18666A (D2), though the overall amount of cholesterol was not as high as that seen in cells grown in F12 (+10% fetal bovine serum) for 24 h with U18666A (D3). nuc, nucleus; bar, 5 μm. Video 7 accompanies Figure 7B untreated. Movements of perinuclear NPC1-FP organelles in untreated cells. Images were acquired approximately every 0.25 s for 50 s and played back at a rate of 15 images per second. Video 8 accompanies Figure 7B 3 h U18666A. Decreased movements of perinuclear NPC1-FP organelles in cells following U18666A treatment. Images were acquired approximately every 0.25 s for 25 s and played back at a rate of 15 images per second. Video 6 accompanies Figure 7A. The formation of abnormal organelles in cells treated with U18666A. Images were acquired every 30 s for 2 h and played back at a rate of six images per second.

Vesicular Traffic Out of the NPC1 Compartment that Continues Without Functional NPC1

Traffic out of perinuclear organelles appears to be largely blocked in cells lacking functional NPC1 based on the loss of the rapidly moving NPC1-positive/VAMP7-positive organelles. However, small VAMP7-FP-positive vesicles that lack NPC1 continue to emerge from the enlarged organelles. These VAMP7-FP "dots" move rapidly (up to $\geq$10 μm/s) along the surface of the enlarged cholesterol-laden organelles and appear to be budding off, even in CT60 cells that lack NPC1 function (Figure 8 and video S1). Loss of NPC1 blocks the emergence of only specific structures from the cholesterol-laden organelles.

DISCUSSION

Dynamic Movements of NPC1-bearing Organelles and Transport Functions

In this study DiI tracing, microscopy of living cells, and drug treatments have been applied to the study of NPC1, a protein necessary to prevent a severe neurodegenerative lipid storage disorder. The movements of NPC1-bearing organelles, and how they change in mutant or drug situations,

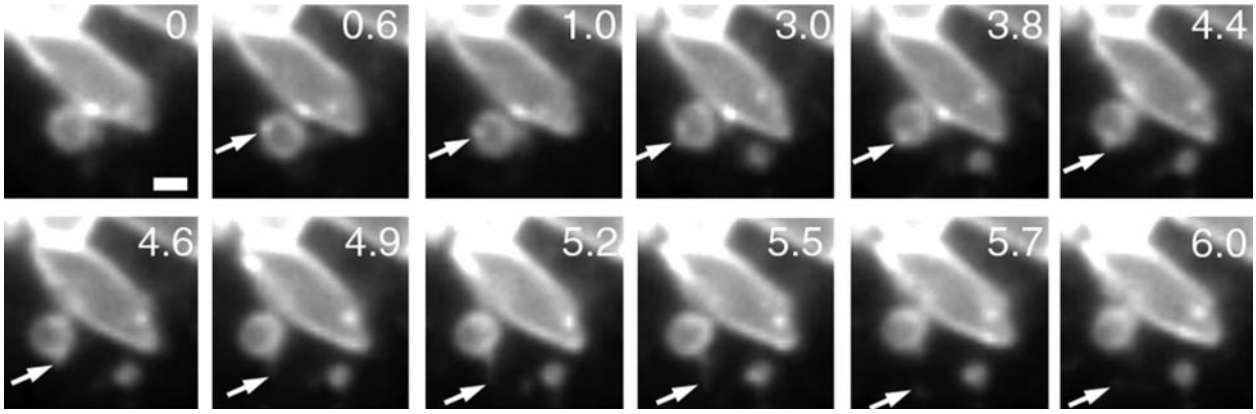

Figure 8. Some vesicular traffic continues out of cholesterol-laden organelles in *NPC1* mutant cells. Images from CT60 cells transiently transfected with VAMP7-YFP were taken using streaming acquisition. VAMP7 localizes to the large abnormal organelles found in NPC, as well as VAMP7-positive, NPC1-negative vesicles that continue to move rapidly without functional NPC1. The arrow at 0.6 s points at a bright VAMP7 spot. At 4.6 s, this structure begins to extend off of the parent organelle. Between 5.5 and 5.7 s, what appears to be a fission event occurs as the tubule is severed. Bar, 1 μm. Video 9 accompanies Figure 8. Continued movement of VAMP7-positive/NPC1-negative vesicles out of cholesterol-laden organelles. Images were acquired every 0.25 s for 6 s and were played back at a rate of four images per second.

offer clues about NPC1 function. We characterized the movements of NPC1 organelles to provide a baseline set of normal cellular activities in which these organelles participate. Then, by examining the movements in cells lacking functional NPC1, we determined that the dramatic vectorial movements were decreased while other movements were not affected. Using the drug U18666A we were able to observe the progression of cellular events that leads to an NPC1-like phenotype.

NPC1-FP organelles are engaged in fast, vectorial movements between more stable peripheral and perinuclear membranous aggregates. The buildup of cholesterol in NPC1 mutant cells could be related to flaws in this movement. A current view of cholesterol uptake is that LDL is delivered by the endocytic pathway to lysosomes, and then cholesterol moves from the lysosomes primarily via the plasma membrane to the ER (Liscum and Munn, 1999). How might NPC1 organelle movement be related to this pathway? In NPC1 mutant cells cholesterol accumulates in late endosome or lysosome-like organelles, indicating a possible block in transport to the plasma membrane. NPC1-bearing transport vesicles could carry cholesterol from lysosomes to the plasma membrane (Liscum and Munn, 1999; Neufeld *et al.*, 1999), though we observed no fusions between NPC1 organelles and the plasma membrane. A second route of trafficking from lysosomes to the plasma membrane could be facilitated by the small VAMP7-positive, NPC1-negative structures. In fact, Lafont *et al.* (1999) showed that VAMP7 is in sphingolipid-cholesterol rich "rafts" that move to the apical plasma membrane. The continued budding of VAMP7-positive structures out of the enlarged cholesterol-laden organelles could explain why a recent study showed no defect in lysosome to plasma membrane movement of cholesterol in NPC1 mutant cells (Lange *et al.*, 2000). The movements of VAMP7-positive/NPC1-negative vesicles indicate that loss of NPC1 function prevents only a subset of the movements out of the perinuclear NPC organelles. The NPC1 mutation therefore discriminates between finely controlled aspects of organelle export.

ther studies have suggested a cholesterol transport route from lysosomes to the ER that does not involve the plasma membrane (Neufeld *et al.*, 1996; Underwood *et al.*, 1998). The ER is clearly affected by loss of NPC1 function, since *NPC1* mutant cells fail to make an appropriate homeostatic response to excess cholesterol. Normally, cholesterol levels are sensed by sterol-sensitive proteins embedded in the ER, including SCAP and HMG-CoA reductase (Brown and Goldstein, 1999). Our two-color time-lapse experiments revealed a close association between NPC1-bearing organelles and parts of the ER.

One possible consequence of this association is that it allows a transfer of cholesterol between NPC1 organelles and the ER. Mutation of *NPC1* would result in lower ER cholesterol content or lower flux of cholesterol through the ER. This would eliminate the homeostatic response to excess cholesterol, as occurs in *NPC1* mutant cells. Another possibility is that changes in the latticework of the ER are guided by the actions of NPC1 organelles. We observe an association of the tips of extending strands of ER with organelles rich in NPC1. A possibly related phenomenon has been seen before. Allan and Vale (1994) identified "globular domains" at the tips of extending ER strands that appear to be attachment points for motors participating in strand extension. If NPC1 played a critical role in organelles that guide ER strand extension, new contacts between the ER and other membrane compartments could be created or regulated by NPC1. In the absence of NPC1, the failure to make particular ER contacts might prevent SREBP cleavage-activity protein (SCAP) and 3-hydroxy-3-methylglutaryl-CoA reductase from sensing the cell's abundant cholesterol.

NPC1 Function in the Terminal Stages of Endocytosis

In *NPC1* mutant cells, abnormal enlarged cholesterol-laden organelles are formed. The cellular events that lead to the formation of the aberrant organelles are unknown. The movements of the abnormal organelles are severely de-

creased compared with NPC1 organelles in normal cells. Similar changes are caused by U18666A and we used this drug to observe early changes in the dynamics of NPC1 organelles. Confidence in U18666A as a meaningful mimic of NPC1 loss of function is bolstered by our finding that overexpressed NPC1 suppresses the effects of the drug. This is a strong indication that NPC1 may be the target of U18666A or that the two act along the same pathway. For example the drug could inhibit an upstream activator of NPC1, in which case heightened NPC1 could replace the lost upstream regulator.

The first dramatic change in response to U18666A is a decrease in outward vectorial movements of NPC1 organelles. This decrease precedes most of the cholesterol accumulation in cells treated with U18666A, so the diminished movements are, initially at least, not due to the bloating of the organelles. Tubular extensions and movement involving the perinuclear NPC1 organelles are significantly decreased within the first few hours of incubation with the drug. Late endosomes and lysosomes appear to continue to fuse in the perinuclear region, while their exit from the perinuclear organelles may be blocked.

Examining these findings in light of our DiI LDL studies suggests a general role for NPC1 in the late stages of the endocytic pathway. If NPC1 is not working, movements of NPC1 organelles are severely reduced and they accumulate in perinuclear regions. The DiI LDL pulse-chase experiments suggest that these aberrant organelles are most similar to a terminal endocytic compartment. In cells lacking functional NPC1, cholesterol-laden organelles accumulate DiI after a 2-h chase. DiI that reaches these enlarged organelles is trapped there, no longer undergoing vectorial movements. In contrast, in cells with functional NPC1 the DiI continues to engage in vectorial movement after a 2-h chase and even after an overnight chase. Movements that normally occur after endocytic cargo reaches the terminal compartment fail to occur in cells lacking functional NPC1. NPC1 may be involved in partitioning late endosomal and lysosomal components so they can participate in another round of endocytic trafficking and degradation.

NPC1 might control organelle partitioning events by affecting membrane transfer or transport events. A transporter function is suggested by the similarity of the NPC1 sequence and topology to resistance-nodulation-cell division permeases (Tseng *et al.*, 1999). Some members of this family mediate transport of hydrophobic molecules through a proton-antiport mechanism. NPC1 could affect lipid, protein, or small molecule transport to properly partition organelles or their cargoes.

NPC1 might cause vesicles or organelles to bud from hybrid late endosomal/lysosomal organelles. By moving a lipid molecule from one leaflet of the organellar membrane to the other a distortion in the lipid bilayer would be introduced that could act either in vesicle formation or scission. Such a mechanism of action has been demonstrated for MDR2, an ABC transporter that functions as a "flippase" to move phosphatidlycholine from one leaflet to the other, possibly causing budding of vesicles within the canalicular space (Ruetz and Gros, 1994). Other proteins related by sequence to NPC1 could function in analogous ways. The SCAP transmembrane protein, a sterol sensor critical for cholesterol homeostasis, escorts sterol regulatory element-binding proteins (SREBPs) from the ER to the Golgi under conditions of low sterols (Nohturfft *et al.*, 1999). SCAP could facilitate budding of ER-to-Golgi transport vesicles.

The dynamic movements of NPC1 organelles, movements that we find depend upon NPC1 function, must be critical for maintaining cell homeostasis. Learning how NPC1 affects membrane compartments and transport events is important for understanding cell functions and for developing new approaches to preventing or healing NPC1 disease.

ACKNOWLEDGMENTS

We are grateful to the Ara Parseghian Foundation for their support of this research. We thank Jamie White, Raj Advani, Stacie Loftus, Jonathan Cruz, T.Y. Chang, Suzanne Pfeffer, and Sherman Garver for plasmids and other materials. We thank James Nelson, Soumya Raychaudhuri, Richard Scheller, Robert Simoni, and Limin Zheng for comments on the manuscript. D.C.K. was supported by a Medical Scientist Training Grant. M.P.S. is an Investigator of the Howard Hughes Medical Institute.

REFERENCES

Advani, R.J., Bae, H.R., Bock, J.B., Chao, D.S., Doung, Y.C., Prekeris, R., Yoo, J.S., and Scheller, R.H. (1998). Seven novel mammalian SNARE proteins localize to distinct membrane compartments. J. Biol. Chem. *273*, 10317–10324.

Advani, R.J., Yang, B., Prekeris, R., Lee, K.C., Klumperman, J., and Scheller, R.H. (1999). VAMP-7 mediates vesicular transport from endosomes to lysosomes. J. Cell Biol. *146*, 765–776.

Allan, V., and Vale, R. (1994). Movement of membrane tubules along microtubules in vitro: evidence for specialized sites of motor attachment. J. Cell Sci. *107*, 1885–1897.

Blanchette-Mackie, E.J., Dwyer, N.K., Amende, L.M., Kruth, H.S., Butler, J.D., Sokol, J., Comly, M.E., Vanier, M.T., August, J.T., Brady, R.O., and et al. (1988). Type-C Niemann-Pick disease: low density lipoprotein uptake is associated with premature cholesterol accumulation in the Golgi complex and excessive cholesterol storage in lysosomes. Proc. Natl. Acad. Sci. USA *85*, 8022–8026.

Brown, M.S., and Goldstein, J.L. (1999). A proteolytic pathway that controls the cholesterol content of membranes, cells, and blood. Proc. Natl. Acad. Sci. USA *96*, 11041–11048.

Butler, J.D., Blanchette-Mackie, J., Goldin, E., O'Neill, R.R., Carstea, G., Roff, C.F., Patterson, M.C., Patel, S., Comly, M.E., and Cooney, A. (1992). Progesterone blocks cholesterol translocation from lysosomes. J. Biol. Chem. *267*, 23797–23805.

Cadigan, K.M., Heider, J.G., and Chang, T.Y. (1988). Isolation and characterization of Chinese hamster ovary cell mutants deficient in acyl-coenzyme A:cholesterol acyltransferase activity. J. Biol. Chem. *263*, 274–282.

Cadigan, K.M., Spillane, D.M., and Chang, T.Y. (1990). Isolation and characterization of Chinese hamster ovary cell mutants defective in intracellular low density lipoprotein-cholesterol trafficking. J. Cell Biol. *110*, 295–308.

Carstea, E.D., Morris, J.A., Coleman, K.G., Loftus, S.K., Zhang, D., Cummings, C., Gu, J., Rosenfeld, M.A., Pavan, W.J., Krizman, D.B., Nagle, J., Polymeropoulos, M.H., Sturley, S.L., Ioannou, Y.A., Higgins, M.E., Comly, M., Cooney, A., Brown, A., Kaneski, C.R., Blanchette-Mackie, E.J., Dwyer, N.K., Neufeld, E.B., Chang, T.Y., Liscum, L., Strauss, J.F., Ohno, K., Zeigler, M., Carmi, R., Sokol, J., Markie, D., O'Neill, R.R., Van Diggelen, O.P., Elleder, M., Patterson, M.C., Brady, R.O., Vanier, M.T., Peutcher, P.G., and Tagle, D.A. (1997). Niemann-Pick C1 disease gene: homology to mediators of cholesterol homeostasis. Science *277*, 228–231.

Cruz, J.C., Sugii, S., Yu, C., and Chang, T.Y. (2000). Role of Niemann-Pick type C1 protein in intracellular trafficking of low density lipoprotein-derived cholesterol. J. Biol. Chem. *275*, 4013–4021.

Herman, B., and Albertini, D.F. (1984). A time-lapse video image intensification analysis of cytoplasmic organelle movements during endosome translocation. J. Cell Biol. *98*, 565–576.

Higgins, M.E., Davies, J.P., Chen, F.W., and Ioannou, Y.A. (1999). Niemann-Pick C1 is a late endosome-resident protein that transiently associates with lysosomes and the trans-Golgi network. Mol. Genet. Metab. *68*, 1–13.

Kobayashi, T., Beuchat, M.H., Lindsay, M., Frias, S., Palmiter, R.D., Sakuraba, H., Parton, R.G., and Gruenberg, J. (1999). Late endosomal membranes rich in lysobisphosphatidic acid regulate cholesterol transport [see comments]. Nat. Cell Biol. *1*, 113–118.

Lafont, F., Verkade, P., Galli, T., Wimmer, C., Louvard, D., and Simons, K. (1999). Raft association of SNAP receptors acting in apical trafficking in Madin-Darby canine kidney cells. Proc. Natl. Acad. Sci. USA *96*, 3734–3738.

Lange, Y., Ye, J., Rigney, M., and Steck, T. (2000). Cholesterol movement in Niemann-Pick type C cells and in cells treated with amphiphiles. J. Biol. Chem. *275*, 17468–17475.

Liscum, L., and Faust, J.R. (1987). Low density lipoprotein (LDL)-mediated suppression of cholesterol synthesis and LDL uptake is defective in Niemann-Pick type C fibroblasts. *J. Biol. Chem*. *262*, 17002–17008.

Liscum, L., and Munn, N.J. (1999). Intracellular cholesterol transport. Biochim. Biophys. Acta *1438*, 19–37.

Liscum, L., Ruggiero, R.M., and Faust, J.R. (1989). The intracellular transport of low density lipoprotein-derived cholesterol is defective in Niemann-Pick type C fibroblasts. J. Cell Biol. *108*, 1625–1636.

Luzio, J.P., Rous, B.A., Bright, N.A., Pryor, P.R., Mullock, B.M., and Piper, R.C. (2000). Lysosome-endosome fusion and lysosome biogenesis. J. Cell Sci. *113*, 1515–1524.

Matteoni, R., and Kreis, T.E. (1987). Translocation and clustering of endosomes and lysosomes depends on microtubules. J. Cell Biol. *105*, 1253–1265.

Neufeld, E.B., Cooney, A.M., Pitha, J., Dawidowicz, E.A., Dwyer, N.K., Pentchev, P.G., and Blanchette-Mackie, E.J. (1996). Intracellular trafficking of cholesterol monitored with a cyclodextrin. J. Biol. Chem. *271*, 21604–21613.

Neufeld, E.B., Wastney, M., Patel, S., Suresh, S., Cooney, A.M., Dwyer, N.K., Roff, C.F., Ohno, K., Morris, J.A., Carstea, E.D., Incardona, J.P., Strauss, J.F., III, Vanier, M.T., Patterson, M.C., Brady, R.O., Pentchev, P.G., and Blanchette-Mackie, E.J. (1999). The Niemann-Pick C1 protein resides in a vesicular compartment linked to retrograde transport of multiple lysosomal cargo. J. Biol. Chem. *274*, 9627–9635.

Nohturfft, A., DeBose-Boyd, R.A., Scheek, S., Goldstein, J.L., and Brown, M.S. (1999). Sterols regulate cycling of SREBP cleavage-activating protein (SCAP) between endoplasmic reticulum and Golgi. Proc. Natl. Acad. Sci. USA *96*, 11235–11240.

Ohashi, M., Murata, M., and Ohnishi, S. (1992). A novel fluorescence method to monitor the lysosomal disintegration of low density lipoprotein. Eur. J. Cell Biol. *59*, 116–126.

Pentchev, P.G., Boothe, A.D., Kruth, H.S., Weintroub, H., Stivers, J., and Brady, R.O. (1984). A genetic storage disorder in BALB/C mice with a metabolic block in esterification of exogenous cholesterol. J. Biol. Chem. *259*, 5784–5791.

Pentchev, P.G., M.E. Comly, H.S. Kruth, T. Tokoro, J. Butler, J. Sokol, M. Filling-Katz, J.M. Quirk, D.C. Marshall, S. Patel, and et al. 1987. Group C Niemann-Pick disease: faulty regulation of low-density lipoprotein uptake and cholesterol storage in cultured fibroblasts. FASEB J. *1*, 40–45.

Pentchev, P.G., Vanier, M.T., Suzuki, K., and Patterson, M.C. (1995). Niemann-Pick disease type C: a cellular cholesterol lipidosis. In: The Metabolic and Molecular Bases of Inherited Disease, vol. II, ed. C.R. Scriver, A.L. Beaudet, W.S. Sly, and D. Valle, New York: McGraw Hill, 2625–2639.

Puri, V., Watanabe, R., Dominguez, M., Sun, X., Wheatley, C.L., Marks, D.L., and Pagano, R.E. (1999). Cholesterol modulates membrane traffic along the endocytic pathway in sphingolipid-storage diseases. Nat. Cell Biol. *1*, 386–388.

Rolls, M.M., Stein, P.A., Taylor, S.S., Ha, E., McKeon, F., and Rapoport, T.A. (1999). A visual screen of a GFP-fusion library identifies a new type of nuclear envelope membrane protein. J. Cell Biol. *146*, 29–44.

Ruetz, S., and Gros, P. (1994). Phosphatidylcholine translocase: a physiological role for the mdr2 gene. Cell *77*, 1071–1081.

Salzman, N.H., and Maxfield, F.R. (1989). Fusion accessibility of endocytic compartments along the recycling and lysosomal endocytic pathways in intact cells. J. Cell Biol. *109*, 2097–2104.

Sokol, J., Blanchette-Mackie, J., Kruth, H.S., Dwyer, N.K., Amende, L.M., Butler, J.D., Robinson, E., Patel, S., Brady, R.O., and Comly, M.E. (1988). Type C Niemann-Pick disease. Lysosomal accumulation and defective intracellular mobilization of low density lipoprotein cholesterol. J. Biol. Chem. *263*, 3411–3417.

Storrie, B., White, J., Rottger, S., Stelzer, E.H., Suganuma, T., and Nilsson, T. (1998). Recycling of golgi-resident glycosyltransferases through the ER reveals a novel pathway and provides an explanation for nocodazole-induced Golgi scattering. J. Cell Biol. *143*, 1505–1521.

Toomre, D., Keller, P., White, J., Olivo, J.C., and Simons, K. (1999). Dual-color visualization of trans-Golgi network to plasma membrane traffic along microtubules in living cells. J. Cell Sci. *112*, 21–33.

Tseng, T.T., Gratwick, K.S., Kollman, J., Park, D., Nies, D.H., Goffeau, A., and Saier, M.H., Jr. (1999). The RND permease superfamily: an ancient, ubiquitous and diverse family that includes human disease and development proteins. J. Mol. Microbiol. Biotechnol. *1*, 107–125.

Underwood, K.W., Jacobs, N.L., Howley, A., and Liscum, L. (1998). Evidence for a cholesterol transport pathway from lysosomes to endoplasmic reticulum that is independent of the plasma membrane. J. Biol. Chem. *273*, 4266–4274.

Watanabe, Y., Akaboshi, S., Ishida, G., Takeshima, T., Yano, T., Taniguchi, M., Ohno, K., and Nakashima, K. (1998). Increased levels of GM2 ganglioside in fibroblasts from a patient with juvenile Niemann-Pick disease type C. Brain. Dev. *20*, 95–97.

Watari, H., Blanchette-Mackie, E.J., Dwyer, N.K., Glick, J.M., Patel, S., Neufeld, E.B., Brady, R.O., Pentchev, P.G., and Strauss, J.F., III. (1999a). Niemann-Pick C1 protein: obligatory roles for N-terminal domains and lysosomal targeting in cholesterol mobilization. Proc. Natl. Acad. Sci. USA *96*, 805–810.

Watari, H., Blanchette-Mackie, E.J., Dwyer, N.K., Watari, M., Neufeld, E.B., Patel, S., Pentchev, P.G., and Strauss, J.F., III. (1999b). Mutations in the leucine zipper motif and sterol-sensing domain inactivate the Niemann-Pick C1 glycoprotein. J. Biol. Chem. *274*, 21861–21866.